J Mol Model (2014) 20:2545
DOI 10.1007/s00894-014-2545-5

ORIGINAL PAPER

An ab initio study on the concerted interaction between chalcogen and pnicogen bonds

Bahman Mohammadian Asiabar · Mehdi D. Esrafili · Fariba Mohammadian-Sabet · Hamid Reza Sobhi · Majid Javaheri

Received: 12 October 2014 / Accepted: 24 November 2014 / Published online: 11 December 2014

Abstract We analyzed cooperation between chalcogen-bonding and pnicogen-bonding interactions in $XHS\cdots NCH_2P\cdots NCY$ (X=F, Cl; Y=H, OH, NH_2, CN and NC) complexes at the MP2/6–311++G** level. These effects were studied in terms of geometric and energetic properties, harmonic frequencies, and nuclear magnetic resonance (NMR). A cooperativity factor was adopted to measure the cooperativity between the two types of interaction in triads based on S–X and P–CN stretching frequencies. The size of the cooperative effect in each complex depends on the strength of S···N and P···N interactions. It is largest for $FHSN\cdots CH_2P\cdots NCNH_2$ and smallest for $ClHS\cdots NCH_2P\cdots NCCN$ and $ClHS\cdots NCH_2P\cdots NCNC$ complexes. The total spin–spin coupling constants across the chalcogen and pnicogen bonds in the ternary complexes are always larger than those in the binary systems. This trend can be also interpreted as a cooperative effect between chalcogen and pnicogen bond interactions. The enhancing mechanism was analyzed in terms of electron redistribution effects in $XHS\cdots NCH_2P\cdots NCY$ complexes.

Keywords Pnicogen bond · Chalcogen bond · Cooperativity · IR stretching frequency · Spin–spin coupling constants

B. M. Asiabar
Department of Chemistry, Faculty of Science, Imam Ali University, Tehran, Iran

M. D. Esrafili (✉) · F. Mohammadian-Sabet
Laboratory of Theoretical Chemistry, Department of Chemistry, University of Maragheh, Maragheh, Iran
e-mail: esrafili@maragheh.ac.ir

H. R. Sobhi
Department of Chemistry, Payame Noor University, Tehran, Iran

M. Javaheri
School of Chemistry, University College of Science, University of Tehran, Tehran, Iran

Introduction

The understanding and control of noncovalent interactions plays a key role in supramolecular chemistry and biological systems. Noncovalent interactions are the main interactions responsible for the properties of condensed phases, solutions, and crystals [1–4]. The classical hydrogen bond—an example of a strong intermolecular interaction—has been studied extensively from both theoretical and experimental viewpoints [5, 6]. Hydrogen bond interactions are defined most frequently as an A–H·B attraction, where A and B are electronegative elements and B possesses one or more lone electron pairs. However, there are also so-called unconventional hydrogen bonds such as C–H·B hydrogen bonds [7], blue-shifting hydrogen bonds [8], π-hydrogen bonds [9], and single-electron hydrogen bonds [10]. While hydrogen-bonding has long been acknowledged however, considerable attention has been paid recently to other intermolecular interactions. Currently, halogen-bonding [11–13] is one such interaction that is being investigated intensively, since it has been found to share many properties with hydrogen bonds [14, 15]. A halogen bond is defined as an attractive R–X B interaction where the halogen X acts as a Lewis acid and B is any site with an excess of electron charge density, most often being an atom with an electron lone-pair. In the literature, the occurrence of halogen bonds is explained in terms of a region of positive electrostatic potential that is present along the outermost portions of some covalently bonded halogen atoms. This electron-deficient region was referred to as a "σ-hole" by Politzer et al. [16–25], and its presence allows for the intuitive description of halogen-bonding as an electrostatically driven interaction between the Lewis base and the σ-hole.

Although the σ-hole concept was used initially to rationalize the seeming anomaly of an electronegative halogen interacting attractively with a negative site, it has since been found to be extended also to covalently bonded atoms in

Group VI [26, 27]. This means that chalcogen atoms (O, S, Se and Te) can indeed have regions of positive electrostatic potential on extensions of the covalent bonds to these atoms. Since this positive electrostatic potential arises from the shifting of electronic charge that accompanies the formation of the covalent bond to the chalcogen atom, it can be expected that the σ-hole potential becomes more positive (1) in going from the lighter to the heavier atoms, as polarizability increases and electronegativity decreases (O<S<Se<Te); and (2) as the remainder of the molecule becomes more electron withdrawing. The formation of noncovalent interactions between positive σ-holes on chalcogen atoms and negative sites has been studied extensively computationally [28–30] and many such complexes have also been reported experimentally [31–33]. This interaction was named "chalcogen-bonding" [34] by analogy with halogen-bonding and hydrogen-bonding. Chalcogen-bonding plays important roles in controlling molecular recognition processes in biological systems and determining molecular orientation in the packing of molecules in crystals [35–37]. As in halogen bonds, the dominance of either electrostatic [38] or dispersion [39] contributions to the stabilization energy of the chalcogen bond is evident, although polarization and charge transfer effects seem also to play a significant role in determining the complex structure [40].

The anisotropic distribution of electrostatic potentials is also found for covalently bonded Group V atoms [26, 27]. Therefore, the pnicogen atoms (N, P, As and Sb) can also interact with an electron donor to form a noncovalent interaction, which is similar in nature to the halogen bond. The well-known "pnicogen bond" usually refers to the noncovalent R–Pn···B interaction, in which the pnicogen atom (Pn) acts as a Lewis acid and B is an electron donor [41–43]. Pnicogen bond interactions have been studied widely, both theoretically [44–46] and experimentally [47]. Pnicogen bond interactions are relevant in biological systems. For instance, the P···N pnicogen bond interactions were found in protein β-sheets [48]. Pnicogen bonds involving the Sb atom also likely participate in the mechanism of inhibition of Sb-based drugs used to treat leishmaniasis [49].

In complex systems with the presence of two or more noncovalent interactions, there is a mutual interplay between them, irrespective of whether they are of the same type [50, 51] or different [52–55]. This mutual influence can lead to interesting cooperativity or synergic effects. Thus, the strength of chalcogen bond or pnicogen bond interactions in complexes usually increases as further molecules are added [56–58]; also, the frequencies of some vibrational modes are shifted by effect of the incorporation of new molecule(s). For example, the cooperative effects between pnicogen and halogen bonds were studied by Li and coworkers [59] for $XCl\cdots FH_2P\cdots NH_3$ (X=F, OH, CN, NC, and FCC) complexes. Interestingly, the increased percentage is more prominent for the interaction energy of the halogen bond. The interplay between halogen and chalcogen bond interactions in $F_2S\cdots NCX\cdots NCY$ (X=F, Cl, Br, I; Y=H, F, OH) has been investigated recently [60]. Ab initio calculations revealed that the formation of X···N halogen bond interaction leads to a shorter S···N distance, increased strength of chalcogen bond, and synergistic energetic effects. Due to the similarity between pnicogen and chalcogen bonds, it is believed that a cooperative effect is also present between them. Studying the interplay between the two interactions could be helpful in understanding the mutual influence between them in crystal engineering and molecular recognition.

Careful studies of simple models are of interest in order to extend their conclusions to larger ones. The main objective of the present study was to examine the cooperative effect of chalcogen and pnicogen bonds on selected properties of $XHS\cdots NCH_2P\cdots NCY$ complexes, where X=F, Cl and Y=H, OH, NH_2, CN, NC. A detailed analysis of the binding distances, interaction energies, harmonic vibrational frequencies and nuclear magnetic resonance (NMR) properties of these complexes was performed. The mechanism of cooperative effects was unveiled by energy decomposition analysis and molecular electrostatic potentials. According to our literature survey, no theoretical investigations concerning this issue are available to date. The results of this study could be very helpful in crystal engineering and molecular recognition, because pnicogen and chalcogen bonds have recently been applied in the design and synthesis of novel functional materials and effective molecular receptors [32, 33, 48].

Computational details

The geometries of all studied complexes were fully optimized at the MP2/6-311++G** level of theory using the GAMESS suite of programs [61]. Harmonic frequency calculations performed at the same level indicated that all the structures obtained correspond to energetic minima. The interaction energies were estimated at the MP2/6-311++G** level with corrections for basis set superposition error (BSSE) using the counterpoise method of Boys and Bernardi [62]. The nature of the interaction was explored using the following energy decomposition analysis [63]:

$$E_{int} = E_{elst} + E_{exch-rep} + E_{pol} + E_{corr} \quad (1)$$

where E_{elst} describes the classical columbic interaction of the occupied orbitals of one monomer with those of another monomer, and $E_{exch\text{-}rep}$ is the sum of the exchange and repulsive energy terms, resulting from the Pauli exclusion principle. E_{pol} is defined as the "orbital relaxation energy" on going from the monomer Hartree-Fock (HF) spin orbitals to the supermolecule HF spin orbitals, and E_{corr} contains all intramolecular electron correlation terms (i.e., electron correlation

correction to the electrostatic, exchange-repulsion and polarization terms) as well as inter-molecular correlation energy.

To further understand the cooperativity between the chalcogen and pnicogen bonds interactions, we performed an analysis of many-body decomposition of the interaction energy [64]. The total interaction energy of a triad (T) equals to the sum of relaxation energy and many-body terms:

$$E_{int}(T) = E_R + E_{2-body} + E_{3-body} \quad (2)$$

where

$$E_{2-body} = E_{int}(12) + E_{int}(23) + E_{int}(13) \quad (3)$$

The relaxation energy (E_R) is defined as the energy sum of the monomers frozen in the geometry of the triads minus the energy sum of the optimized monomers. The two-body terms E_{int} (12), E_{int} (23), and E_{int} (13) can be calculated as the interaction energy of each molecular pair in the geometry of triad minus the energy sum of the monomers, all of them frozen in the geometry of the triad. The three-body term $E_{3\text{-body}}$ is a measure of cooperativity between the two interactions in a ternary system, where a negative $E_{3\text{-body}}$ indicates that the two interactions work in concert with each other and enhance each other's strength.

Molecular electrostatic potentials (MEP) were calculated with wave function analysis–surface analysis suite (WFA–SAS) developed by Politzer and coworkers [65]. Chemical shielding tensors as well as spin–spin coupling constants across the S···N and P···N bonds were computed using the gauge-including atomic orbital (GIAO) approach [66].

Results and discussion

Structures and IR frequencies

The optimized geometry of XHS···NCH_2P···NCY (X=F, Cl and Y=H, OH, NH_2, CN, NC) complexes is illustrated schematically in Fig. 1. For each complex studied, there are two interaction modes. The first is a chalcogen bond formed between the S atom in SHX and the nitrogen atom of PH_2CN. The second is a pnicogen bond through the P atom in PH_2CN as an electron acceptor and the N atom in NCY as an electron donor. The formation of these interactions can be understood using electrostatic potentials. The electrostatic potentials of PH_2CN and SHF and SHCl molecules are indicated in Fig. 2, which figure shows the locations of the different most positive and most negative $V_S(r)$, designated as $V_{S,max}$ and $V_{S,min}$, respectively. Looking at the potentials on the surfaces of PH_2CN molecule (Fig. 2), it is evident that the P atom has a buildup of positive potentials on its surface, along the extension of the P–C bond. This positive region corresponds to the σ-hole, because it is centered on the P–C axis and is surrounded by negative electrostatic potential. The $V_{S,max}$ is 43.8 kcal mol^{-1}. There is also a negative potential $V_{S,min}$ associated with the N atom of PH_2CN. This $V_{S,min}$ is about −36.8 kcal mol^{-1}, which is distinctly smaller than that of the nitrogen atom in the NH_3 (−42.7 kcal mol^{-1}). From Fig. 2, it is evident that the sulfur atom in SHF and SHCl molecules also has a region of very positive potential, the σ-hole, with a $V_{S,max}$ value of 52.3 (SHF) and 38.8 kcal mol^{-1} (SHCl) that is located approximately at the extension of the S–F and S–Cl covalent bonds. These positive regions can interact with any negative site, thereby giving rise to a directional interaction. Thus, the noncovalent bonds in these systems are all σ-hole bonds, and the nature of these is no different than that of halogen or hydrogen bonding [26, 27, 67].

The S···N and P···N distances of the XHS···NCH_2P···NCY complexes are summarized in Table 1. Corresponding data for XHS···NCH_2P and NCH_2P···NCY dyads are also reported for comparative purposes. All binary and ternary complexes have a nearly linear structure with C1 symmetry (Fig. 1). The S···N binding distances in the triads range from 2.683 Å in FHS···NCH_2P···$NCNH_2$ to 3.194 Å in ClHS···NCH_2P···NCCN. For a given Y substitution, the S···N distance in the FHS complex is smaller than that in the ClHS complex, which is consistent with the positive electrostatic potentials on the S atoms. The S···N binding distance becomes shorter when the electron-donating ability of the Y group increases. The intermolecular P···N distances between the NCH_2P and NCY molecules in the triads are between 3.004–3.159 and 3.014–3.165 Å for X=F and Cl, respectively. These are comparable to pnicogen bond distances in HOCl···PH_2F, and HOI···PH_2F complexes [68]. Linear relationships are found between the P···N and S···N distances in the ternary complexes (Fig. 3), with the squared correlation coefficient, R^2, having values of 0.976 and 0.974 for X=F and Cl, respectively.

As can be seen from Table 1, the equilibrium binding distances S···N and P···N in the triads are always shorter than those in the respective dyads. The shortening of the S···N distance varies from 0.017 Å in the ClHS···NCH_2P···NCCN

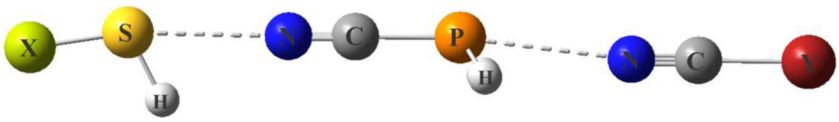

Fig. 1 Structure of XHS···NCH_2P···NCY (X=F, Cl, Y=H, OH, NH_2, NC, CN) triads

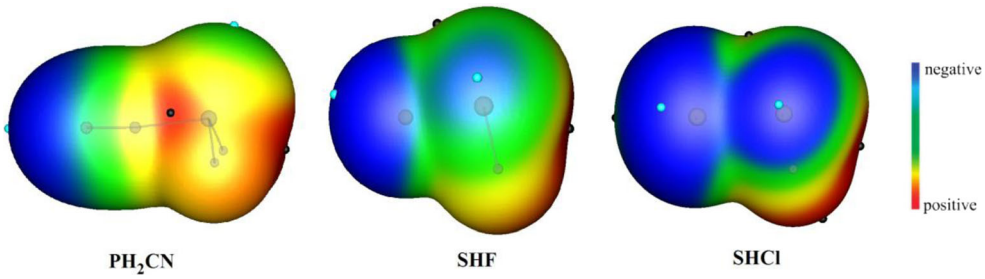

Fig. 2 Electrostatic potentials on the 0.001 a.u. electron density isosurfaces of PH_2CN, SHF and SHCl molecules. *Black circles* Surface maxima, *blue circles* surface minima

to 0.040 Å in the FHS···NCH_2P···$NCNH_2$, while the shortening of the P···N distance is in the range of 0.029–0.050 Å. This can be interpreted as a cooperative (or synergic) effect between the chalcogen and pnicogen bonds in these systems. The shortening effect is larger in the FHS complexes than in the corresponding ClHS ones. Moreover, the effect is larger in complexes with shorter intermolecular distances than in those with the longest ones. This supports the view that the degree of cooperativity is proportional to strength of the intermolecular interactions [52, 53].

Upon formation of chalcogen and pnicogen bonds, the S–X and P–CN bonds are elongated, accompanied by a shift in the S–X and P–CN stretch frequencies, respectively. The calculated vibrational frequencies shifts for the S–X and P–CN stretching modes of the complexes are listed in Table 2. It is evident that the formation of the XHS···NCH_2P complexes results in a red-shift of the S–X stretching vibration in the infrared spectra. The S–F stretch shift in the SHF complex is more prominent than that of the S–Cl bond in the SHCl counterpart, and the bond elongation in the former is larger than that in the latter. This is due to the larger atomic mass of halogen. Cooperative effects strengthen the S···N interactions and therefore lead to a further red-shift in the S–X frequency. In the pnicogen-bonded complexes, the associated P–CN bond stretch shows also a red-shift. Notice, however, that in the triads, the elongation of the corresponding bond length and the red-shifted value of the stretching mode are smaller than those of dyads (Table 2). This may be because P–CN bond elongation is a combinative result of S···N and P···N interactions in the triads. This indicates that the formation of the S···N chalcogen bond after the addition of SHX slightly strengthens the P–CN bond in NCH_2P···NCY. Meanwhile, the amount of red-shift of P–CN in each complex depends on the strength of P···N and S···N interactions. It is largest for FHS···NCH_2P···$NCNH_2$ and smallest for the ClHS···NCH_2P···NCCN and ClHS···NCH_2P···NCNC complexes. This can be considered as evidence for the interplay between the chalcogen and pnicogen bonds.

In the present study, a cooperativity factor (A) [69] was adopted to measure the cooperativity between both interactions in the triads. It was calculated as $A=\Delta\nu\,(T)/\Delta\nu$ where $\Delta\nu$ (T) and $\Delta\nu$ are the frequency shifts in the ternary and binary systems, respectively. The results are listed in Table 3. It can be seen that the cooperativity factor ranges from 1.09 to 1.24 (for ν_{S-X}) and from 0.75 to 0.94 (for ν_{P-CN}). For each series, the cooperativity factor is largest for strongest and smallest for weakest complex. However, the cooperativity factors obtained in this study are much less than those found for the H_3N···XY···HF (X,Y=F, Cl, Br) triads involving halogen and hydrogen bonds [70].

Table 1 Optimized binding distances (R, Å) of chalcogen bond (CB) and pnicogen bond (PB) interactions in the dyads and triads (T)

Complex	R_{CB}	R_{CB} (T)	R_{PB}	R_{PB} (T)
FHS···NCH_2P···NCH	2.723	2.694	3.145	3.102
FHS···NCH_2P···NCOH	2.723	2.689	3.087	3.041
FHS···NCH_2P···$NCNH_2$	2.723	2.683	3.054	3.004
FHS···NCH_2P···NCCN	2.723	2.705	3.194	3.159
FHS···NCH_2P···NCNC	2.723	2.703	3.183	3.144
ClHS···NCH_2P···NCH	2.894	2.867	3.145	3.110
ClHS···NCH_2P···NCOH	2.894	2.862	3.087	3.050
ClHS···NCH_2P···$NCNH_2$	2.894	2.857	3.054	3.014
ClHS···NCH_2P···NCCN	2.894	2.877	3.194	3.165
ClHS···NCH_2P···NCNC	2.894	2.876	3.183	3.151

Interaction energies

The interaction energy has been used widely in the study of the interplay between two kinds of noncovalent interactions. The interaction energies in the binary and ternary complexes

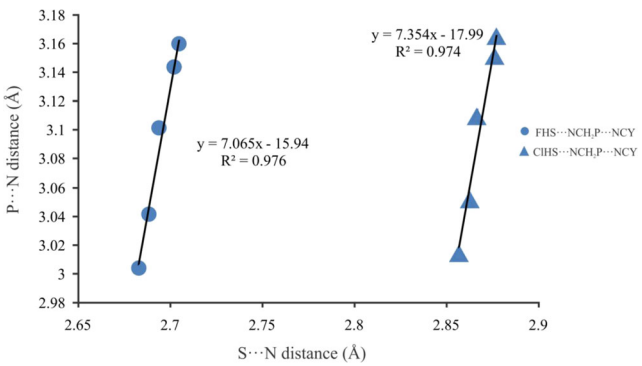

Fig. 3 Correlation between S···N and P···N binding distances in XHS···NCH_2P···NCY triads

Table 2 Calculated S–X and P–CN stretching frequencies shifts (in cm^{-1}) for dyads and triads (T), and cooperativity factor [a,b]

Complex	$\Delta\nu_{S-F/Cl}$	$\Delta\nu_{S-F/Cl}$ (T)	$\Delta\nu_{P-CN}$	$\Delta\nu_{P-CN}$ (T)	A $_{S-F/Cl}$	A $_{P-CN}$
FHS···NCH_2P···NCH	−34	−40	−12	−10	1.18	0.83
FHS···NCH_2P···NCOH	−34	−41	−15	−13	1.21	0.87
FHS···NCH_2P···$NCNH_2$	−34	−42	−17	−16	1.24	0.94
FHS···NCH_2P···NCCN	−34	−37	−8	−6	1.09	0.75
FHS···NCH_2P···NCNC	−34	−37	−8	−6	1.09	0.75
ClHS···NCH_2P···NCH	−15	−18	−12	−6	1.20	0.83
ClHS···NCH_2P···NCOH	−15	−19	−15	−6	1.27	0.87
ClHS···NCH_2P···$NCNH_2$	−15	−19	−17	−10	1.27	0.94
ClHS···NCH_2P···NCCN	−15	−17	−8	−13	1.13	0.75
ClHS···NCH_2P···NCNC	−15	−17	−8	−16	1.13	0.75

[a] A=Δν (T)/Δν

[b] Corresponding harmonic frequencies for isolated PH_2CN, SHF and SHCl molecules are 629, 741 and 528 cm^{-1}, respectively

were obtained as the energy difference between the complex and sum of the isolated monomers. All interaction energies were corrected for the BSSE using the counterpoise method (Table 3). The interaction energies of chalcogen bonds are −4.77 and−3.29 kcal mol^{-1} in FHS···NCH_2P and ClHS···NCH_2P dyads, respectively, which are consistent with the evaluated positive electrostatic potentials on the S atom. As evident from Table 3, the range of interaction energies of NCH_2P···NCY dyads is relatively narrow, from −2.00 to −4.19 kcal mol^{-1}. The pnicogen bond energies in the binary systems vary in the order NH_2>OH>H>NC>CN. This ordering corresponds to the relative magnitudes of the negative electrostatic potentials associated with the nitrogen atom of NCY. The triad interaction energies range from −7.10 to −9.85 kcal mol^{-1} for FHS···NCH_2P···NCY and from −5.51 to−8.10 kcal mol^{-1} for ClHS···NCH_2P···NCY complexes. For each series, the presence of electron-donating groups (Y=OH and NH_2) on the NCY results in more negative interaction energies while the electron-withdrawing substituents (Y=CN and NC) lead to smaller E_{int} (less negative) values.

Table 3 summarizes the evaluated cooperativity energy (E_{coop}), which is intended to provide an estimation of the "extra" energetic stabilization obtained in a multicomponent complex as a consequence of the coexistence of both interactions. It is computed with formulas of $E_{coop}=E_{int}$ (T) $-E_{int}$ (CB)$-E_{int}$ (PB), where E_{int} (T) is the total interaction of the triad, E_{int} (CB) and E_{int} (PB) are the interaction energies of the isolated chalcogen and pnicogen bonded dyads within their corresponding minima configurations. One can see that the estimated values of E_{coop} are all negative, with the maximum and minimum energetic cooperativity values corresponding to the most and least stable complexes, respectively. In the ternary systems, the interaction energy of chalcogen bonding is increased by 15–22 %, whereas that of pnicogen bonding is increased by about 24–40 %. The increase of the latter is much greater than that of the former. It is demonstrated that the effect of the stronger interaction on the weaker one is prominent.

Table 3 Interaction energies (E_{int}, kcal mol^{-1}) of chalcogen bond (CB) and pnicogen bond (PB) interactions in the dyads and triads (T), cooperative energies (E_{coop}, kcal mol^{-1}), and many body analysis for XHS···NCH_2P···NCY complexes

Complex	E_{int} (CB)	E_{int} (PB)	E_{int} (T)	E_{coop}	E_R	E_{int} (12)	E_{int} (23)	E_{int} (13)	E $_{3\text{-body}}$
FHS···NCH_2P···NCH	−4.77	−3.13	−8.53	−0.63	0.04	−4.74	−3.10	−0.18	−0.55
FHS···NCH_2P···NCOH	−4.77	−3.66	−9.19	−0.75	0.06	−4.76	−3.64	−0.21	−0.64
FHS···NCH_2P···$NCNH_2$	−4.77	−4.19	−9.85	−0.88	0.09	−4.76	−4.16	−0.26	−0.76
FHS···NCH_2P···NCCN	−4.77	−2.00	−7.10	−0.32	0.03	−4.75	−1.98	−0.07	−0.33
FHS···NCH_2P···NCNC	−4.77	−2.19	−7.33	−0.37	0.03	−4.75	−2.16	−0.08	−0.37
ClHS···NCH_2P···NCH	−3.29	−3.13	−6.86	−0.44	0.04	−3.23	−3.11	−0.13	−0.43
ClHS···NCH_2P···NCOH	−3.29	−3.66	−7.47	−0.52	0.06	−3.24	−3.64	−0.14	−0.51
ClHS···NCH_2P···$NCNH_2$	−3.29	−4.19	−8.10	−0.61	0.08	−3.25	−4.17	−0.18	−0.58
ClHS···NCH_2P···NCCN	−3.29	−2.00	−5.51	−0.22	0.02	−3.26	−1.98	−0.05	−0.24
ClHS···NCH_2P···NCNC	−3.29	−2.19	−5.73	−0.25	0.03	−3.26	−2.16	−0.06	−0.28

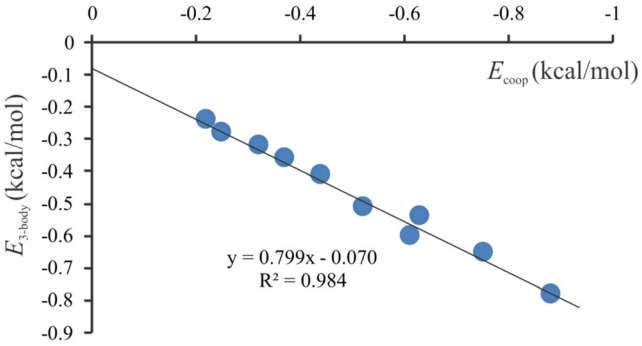

Fig. 4 Relationship between cooperative energy and three-body interaction energy

Table 3 lists the results of the many body interaction energy analyses of the triads. These data indicate that the monomer relaxation energy, E_R, is relatively small at no more than 0.1 kcal mol^{-1}. For all the ternary complexes, the two-body and three-body interaction energies are attractive, indicating a positive contribution to the interaction energy of complexes. As evident, the most important energy component arises from the two-body interactions which account for 93 % to 96 % of the total interaction energy. The contribution of the three-body energy $E_{3\text{-body}}$ decreases with the electron-withdrawing ability of the substitution Y. An excellent correlation is found between the E_{coop} energies in the ternary complexes and the calculated $E_{3\text{-body}}$ energies with R^2=0.984 (Fig. 4). This indicates that the three-body term $E_{3\text{-body}}$ can be used as a measure of cooperative effects between the two interactions in the ternary systems.

In order to gain insight into the contribution of the different energy terms of the interaction energy, an interaction energy decomposition analysis was performed for the binary and ternary complexes (Table 4). It can be seen that, for the FHS···NCH_2P and ClHS···NCH_2P dyads, the dominant attraction energy originates in the electrostatic term (E_{elst}), which amounts to about 65 % of the total attraction energy. The polarization energy in FHS···NCH_2P is more negative than that of ClHS···NCH_2P, which should be related to the greater dipole moment of FHS than ClHS molecule (2.32 vs 1.69 D). In all of the NCH_2P···NCY complexes studied here, the E_{elst} term is the dominant one in absolute value, providing up to 75 % of the total attractive energy of NCH_2P···$NCNH_2$, while in the weakest complex its contribution is only 60 %. The polarization (E_{pol}) energy, which corresponds to between 15 % and 17 % of the total attractive terms, increases in importance from the weakest complex to the strongest one. Finally, the correlation energy (E_{corr}) term contributes to 8 % of all the attractive terms in the strongest complex and increases its contribution, reaching 12 % in the weakest complexes. In the triads, the various energy terms follow the same trend as the interaction energy of the binary systems. As shown in Table 4, the attractive E_{elst} and E_{pol} components make a major contribution to the interaction energies of triads. Overall, the nature of S···N and P···N σ-hole interactions is no different than that of halogen or hydrogen bonding [26, 27].

Electron density redistribution

It may be noted that formation of the R–X···B pnicogen or chalcogen bond interaction is generally accompanied by some mutual polarization of R–X by the electric field of B, and of B

Table 4 Interaction energy terms (in kcal mol^{-1}) for binary and ternary complexes

Complex	E_{elst}	$E_{exch\text{-}rep}$	E_{pol}	E_{corr}	% E_{elst}	% E_{pol}
FHS···NCH_2P	−9.04	8.95	−3.24	−1.42	66	24
ClHS···NCH_2P	−6.06	6.05	−1.91	−1.36	65	20
NCH_2P···NCH	−4.69	3.16	−0.97	−0.62	75	15
NCH_2P···NCOH	−5.54	3.82	−1.23	−0.70	74	16
NCH_2P···$NCNH_2$	−6.45	4.41	−1.50	−0.64	75	17
NCH_2P···NCCN	−2.68	2.47	−0.66	−1.14	60	15
NCH_2P···NCNC	−3.73	2.66	−0.81	−0.31	77	17
FHS···NCH_2P···NCH	−12.27	12.33	−4.47	−2.65	63	23
FHS···NCH_2P···NCOH	−15.84	14.59	−5.7	−2.17	67	24
FHS···NCH_2P···$NCNH_2$	−17.00	15.50	−6.19	−2.11	67	24
FHS···NCH_2P···NCCN	−14.77	13.58	−5.22	−2.08	67	24
FHS···NCH_2P···NCNC	−13.49	12.66	−4.81	−1.63	68	24
ClHS···NCH_2P···NCH	−9.12	9.16	−2.95	−2.57	62	20
ClHS···NCH_2P···NCOH	−12.45	11.09	−3.99	−2.1	67	22
ClHS···NCH_2P···$NCNH_2$	−13.53	11.91	−4.40	−2.03	68	22
ClHS···NCH_2P···NCCN	−11.45	10.20	−3.57	−2.01	67	21
ClHS···NCH_2P···NCNC	−10.28	9.41	−3.24	−1.59	68	21

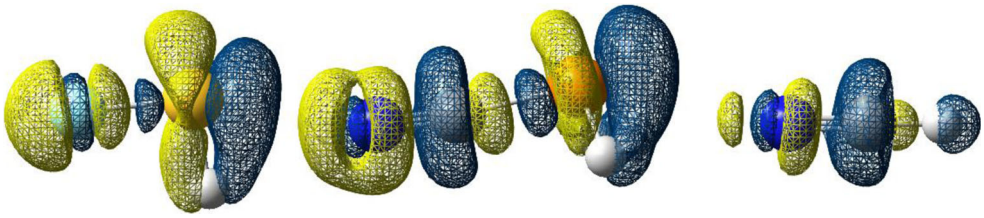

Fig. 5 Electron density difference plot (0.001 a.u.) for the FHS···NCH_2P···NCH complex. *Yellow* Increases in electronic density, *blue* decreases in electronic density

by the electric field of the positive σ-hole on X. This means that electron density on B should become somewhat polarized toward the positive portion of X, and the electron density on X should tend to move away from B. A similar polarization effect has been reported previously for hydrogen and halogen bonds by the groups of Politzer and Clark [23, 26]. Figure 5 indicates the computed electron density difference plot for the complex FHS···NCH_2P···NCH, where loss of electrons is indicated in blue, and electron enrichment is indicated in yellow. It can be seen that there is an increase in electron density between the FHS and NCH_2P surfaces, indicating the formation of the S···N chalcogen bond interaction. The electric field of the positive σ-hole on the S atom of SHX tends to produce a rearrangement of electronic charge within the PH_2CN molecule. It should be noted that the electric field created by the ClHS is relatively weak, due to its small σ-hole (38.8 kcal mol^{-1}). This accordingly results in smaller electronic density shifts around the PH_2CN molecule compared to the FHS. At the same time, the electron density around the area of P atom of PH_2CN that interacts with the NCH unit is decreased. This electron redistribution increases the electric field of the σ-hole on the P atom, so the P···N interaction in the triad is reinforced with respect to the binary NCH_2P···NCH system.

Table 5 The most positive electrostatic potential ($V_{S,max}$, kcal mol^{-1}) and the most negative electrostatic potential ($V_{S,min}$, kcal mol^{-1}) of the monomers and dyads. For each structure, the $V_{S,max}$ or $V_{S,min}$ value is referred to the bold atom

Complex	$V_{S,max}$	$V_{S,min}$
NCH	–	−34.2
NCOH	–	−48.2
NCNH2	–	−42.5
NCCN	–	−19.0
NCNC	–	−10.0
PH2CN	43.8	−36.8
SHF	52.2	–
SHCl	38.9	–
FHS···NCH_2P	50.4	–
ClHS···NCH_2P	49.0	–
NCH_2P···NCH	–	−42.7
NCH_2P···NCOH	–	−43.8
NCH_2P···$NCNH_2$	–	−44.9
NCH_2P···NCCN	–	−39.4
NCH_2P···NCNC	–	−41.3

To further understand the cooperativity between the S···N and P···N interactions in the XHS···NCH_2P···NCY complexes, we calculated the electrostatic potentials of the monomers and corresponding dyads at the MP2/6-311++G** level. As indicated in Table 5, the calculated $V_{S,min}$ on the nitrogen atom of the isolated NCY molecule becomes more negative in the order Y=NC<CN<H<NH_2<OH. Not surprisingly, the presence of electron-donating groups (OH and NH_2) in the NCY molecule causes an increase in the value of $V_{S,min}$, while the electron-withdrawing CN and NC substituents leads to less negative $V_{S,min}$ values. The $V_{S,min}$ value is −36.8 kcal mol^{-1} for the nitrogen atom in PH_2CN monomer. Upon pnicogen bond formation, this value is increased. For example, it is−44.9 kcal mol^{-1} in the H_2NCN···PH_2CN complex. This means that the nitrogen atom of the PH_2CN in the H_2NCN···PH_2CN dyad is a stronger electron donor than that of the isolated molecule, which would enhance the mutual polarization of the PH_2CN and SHX molecules. On the other hand, when SHX interacts with the PH_2CN monomer, the σ-hole potential on the P atom becomes more positive. This demonstrates that the P atom in the PH_2CN is a better electron acceptor than the free PH_2CN molecule. Note that the P atom in FHS···PH_2CN has a relatively larger σ-hole, due to the larger electric field associated with the σ-hole on the S atom in FSH than that of SHCl. Overall, the polarization induced in the PH_2CN by the S···N interaction strengthens the concerted the P···N bond. This demonstrates the importance of the polarization effects in mutual influence between pnicogen and chalcogen bond interactions.

NMR properties

The ^{33}S and ^{31}P absolute chemical shielding values in triads, and their changes relative to binary complexes are given in Table 6. The ^{33}S chemical shielding for FHS···NCH_2P is 284.6 ppm—an increase of 104 ppm relative to the isolated SHF monomer (388.6 ppm). This is a much larger change upon dimer formation than observed for ClHS···NCH_2P (about 5 ppm). The results also indicate that ^{31}P absolute chemical shieldings always decrease in NCH_2P···NCY complexes relative to the corresponding monomer NCH_2P. These decreases range from 1.8 to 4.0 ppm. The largest downshift corresponds to the most strongly bound complexes, i.e., for NCH_2P···$NCNH_2$ and NCH_2P···NCOH complexes, such

Table 6 Absolute ^{33}S and ^{31}P chemical shielding isotropies (σ_{iso}: ppm) and spin-spin coupling constants (Hz) across the chalcogen and pnicogen bonds in XHS···NCH_2P···NCY complexes and the corresponding changes respective to dyads

Complexes	σ_{iso} (^{33}S)	$\Delta\sigma_{iso}$ (^{33}S)	σ_{iso} (^{31}P)	$\Delta\sigma_{iso}$ (^{31}P)	^{1S}J (S–N)	$\Delta^{1S}J$ (S–N)	^{1P}J (P–N)	$\Delta\ ^{1P}J$ (P–N)
FHS···NCH_2P···NCH	278.4	−6.1	492.2	−3.5	11.4	0.4	20.4	0.4
FHS···NCH_2P···NCOH	277.2	−7.3	492.6	−4.2	11.5	0.5	23.6	1.3
FHS···NCH_2P···$NCNH_2$	275.7	−8.9	492.8	−4.6	11.5	0.5	24.7	1.9
FHS···NCH_2P···NCCN	280.6	−4.0	492.0	−2.9	11.2	0.2	20.4	0.4
FHS···NCH_2P···NCNC	280.0	−4.5	492.6	−3.3	11.2	0.2	21.0	0.2
ClHS···NCH_2P···NCH	197.1	−3.3	492.1	−3.2	8.2	0.4	20.4	0.4
ClHS···NCH_2P···NCOH	196.1	−4.2	492.4	−3.6	8.3	0.5	23.3	1.0
ClHS···NCH_2P···$NCNH_2$	195.7	−4.7	812.3	−4.0	8.4	0.6	24.4	1.6
ClHS···NCH_2P···NCCN	199.1	−1.3	491.9	−2.2	8.0	0.2	20.3	0.3
ClHS···NCH_2P···NCNC	198.4	−1.9	492.4	−2.8	8.0	0.2	21.1	0.3

changes amount to 4.0 and 3.8 ppm, respectively. When a SHX molecule is added to the NCH_2P···NCY complex, the calculated ^{31}P absolute chemical shielding is slightly decreased. The amount of this shift depends on the strength of S···N and P···N bonds. It is largest for the strongest and smallest for the weakest complex.

Table 6 lists the total spin-spin coupling constants ^{1S}J (S—N) and ^{1P}J (P–N) across the chalcogen and pnicogen bonds, respectively. All ^{1S}J (S–N) and ^{1P}J (P–N) are positive. One can see that the ^{1S}J (S–N) and ^{1P}J (P–N) values in the ternary complexes are always larger than those in the binary systems. This trend can be also interpreted as a cooperative effect between the chalcogen and pnicogen bond interactions. The ^{1P}J (P–N) is significantly greater than ^{1S}J (S–N), reflecting the dependency of spin-spin coupling constants on the nature of the interaction. The results of Table 6 indicate that the formation of a pnicogen bond interaction has little effect on ^{1S}J (S–N) values of XHS···NCH_2P complexes, increasing their value by 0.2–0.6 Hz. This result confirms that the S···N interactions in the triads are reinforced with respect to binary systems. The corresponding increase in the ^{1P}J (P–N) is more pronounced than those of ^{1S}J (S–N), reflecting the strong cooperative effect of the S···N interaction on the P···N bond. Therefore, this can be understood as an indication of reinforcement of the chalcogen and pnicogen bonds interactions, in agreement with the binding distances and interaction energies discussed above. Figure 6 provides a plot of ^{1S}J (S–N) and ^{1P}J (P–N) versus the S···N and P···N bond distances, respectively. For each case, the trendline shown is a second-order polynomial with a correlation coefficient R^2 of 0.999 (for S···N) and 0.864 (for P···N). These correlations suggest that experimental ^{1S}J (S–N) and ^{1P}J (P–N) values could be used to estimate chalcogen and pnicogen bond distances, respectively.

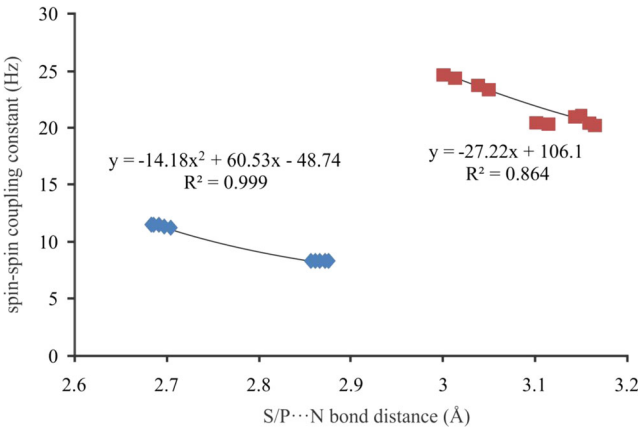

Fig. 6 Spin-spin coupling constants versus chalcogen and pnicogen bond distances

Conclusions

Ab initio calculations at the MP2/6-311++G** level of theory were performed to investigate the mutual influence between the chalcogen bond and pnicogen bond interactions in the XHS···NCH_2P···NCY complexes, where X=F, Cl; Y=H, OH, NH_2, CN and NC. Our results indicated that chalcogen and pnicogen bonds interactions in the title complexes enhance each other, i.e., there is a positive cooperative effect between the monomers. This is confirmed by geometric and energetic parameters; the S(P)···N distance becomes shorter and the interaction energy becomes more negative in the ternary systems. In the ternary systems, the interaction energy of chalcogen bonding is increased by 15–22 %, whereas that of pnicogen bonding is increased by about 24–40 %. The increase of the latter is much greater than that of the former. According to energy decomposition analysis, the attractive E_{elst} and E_{pol} components make the major contribution to the interaction energies of dyads and triads. The variations of the ^{1S}J (S–N) and ^{1P}J (P–N) values in the triads are dependent on the strength of the interaction and they becomes larger in the order Y=NH_2>OH>H>NC>CN.

References

1. Kabeláč M, Hobza P (2007) Hydration and stability of nucleic acid bases and base pairs. Phys Chem Chem Phys 9:903–917
2. Esrafili MD (2008) Behzadi H, Hadipour NL (2008) ^{14}N and ^{17}O electric field gradient tensors in benzamide clusters: theoretical evidence for cooperative and electronic delocalization effects in N–H···O hydrogen bonding. Chem Phys 348:175–180
3. Berka K, Laskowski R, Riley KE, Hobza P, Vondrášek J (2009) Representative amino acid side chain interactions in proteins. A comparison of highly accurate correlated ab initio quantum chemical and empirical potential procedures. J Chem Theory Comput 5:982–992
4. Esrafili MD (2013) Characteristics and nature of the intermolecular interactions in boron-bonded complexes with carbene as electron donor: an ab initio, SAPT and QTAIM study. J Mol Model 18: 2003–2011
5. Jeffrey GA (1997) An introduction to hydrogen bonding. Oxford University Press, Oxford
6. Buckingham AD, Del Bene JE, McDowell SAC (2008) The hydrogen bond. Chem Phys Lett 463:1–10
7. Desiraju GR, Steiner T (1999) The weak hydrogen bond in structural chemistry and biology. Oxford University Press, Oxford
8. Hobza P, Havlas Z (2000) Blue-shifting hydrogen bonds. Chem Rev 100:4253–4264
9. Kim KS, Tarakeshwar P, Lee JY (2000) Molecular clusters of π-systems: theoretical studies of structures, spectra, and origin of interaction energies. Chem Rev 100:4145–4186
10. Wang BQ, Li ZR, Wu D, Hao XY, Li RJ, Sun CC (2003) Single-electron hydrogen bonds in the methyl radical complexes $H_3C\cdots HF$ and $H_3C\cdots HCCH$: an ab initio study. Chem Phys Lett 375:91–95
11. Metrangolo P, Neukirch H, Pilati T, Resnati G (2005) Halogen bonding based recognition processes: a world parallel to hydrogen bonding. Acc Chem Res 38:386–395
12. Politzer P, Murray JS, Concha MC (2007) Halogen bonding and the design of new materials: organic bromides, chlorides and perhaps even fluorides as donors. J Mol Model 13:643–650
13. Riley KE, Hobza P (2008) Investigations into the nature of halogen bonding including symmetry adapted perturbation theory analyses. J Chem Theory Comput 4:232–242
14. Esrafili MD (2013) A theoretical investigation of the characteristics of hydrogen/halogen bonding interactions in dibromo-nitroaniline. J Mol Model 19:1417–1427
15. Aakeröy CB, Fasulo M, Schultheiss N, Desper J, Moore C (2007) Structural competition between hydrogen bonds and halogen bonds. J Am Chem Soc 129:13772–13773
16. Clark T, Hennemann M, Murray JS, Politzer P (2007) Halogen bonding: the σ-hole. J Mol Model 13:291–296
17. Politzer P, Lane P, Concha MC, Ma YG (2007) Murray JS (2007) An overview of halogen bonding. J Mol Model 13:305–311
18. Murray JS, Lane P, Clark T, Politzer P (2007) σ-Hole bonding: molecules containing group VI atoms. J Mol Model 13:1033–1038
19. Murray JS, Lane P, Politzer P (2008) Simultaneous σ-hole and hydrogen bonding by sulfur- and selenium-containing heterocycles. Int J Quantum Chem 108:2770–2781
20. Riley KE, Murray JS, Politzer P, Concha MC, Hobza P (2009) Br···O complexes as probes of factors affecting halogen bonding: interactions of bromobenzenes and bromopyrimidines with acetone. J Chem Theory Comput 5:155–163
21. Politzer P, Murray JS, Clark T (2010) Halogen bonding: an electrostatically-driven highly directional noncovalent interaction. Phys Chem Chem Phys 12:7748–7757
22. Murray JS, Lane P, Clark T, Riley KE, Politzer P (2012) σ-Holes, π-holes and electrostatically-driven interactions. J Mol Model 18:541–548
23. Politzer P, Riley KE, Bulat FA, Murray JS (2012) Perspectives on halogen bonding and other σ-hole interactions: Lex parsimoniae (Occam's Razor). Comput Theor Chem 998:2–8
24. Politzer P, Murray JS (2013) Halogen bonding: an interim discussion. Chem Phys Chem 14:278–294
25. Riley KE, Murray JS, Fanfrlík J, Řezáč J, Solá RJ, Concha MC, Ramos FM, Politzer P (2013) Halogen bond tunability II: the varying roles of electrostatic and dispersion contributions to attraction in halogen bonds. J Mol Model 19:4651–4659
26. Politzer P, Murray JS, Clark T (2013) Halogen bonding and other σ-hole interactions: a perspective. Phys Chem Chem Phys 15:11178–11189
27. Politzer P, Murray JS, Janjić GV, Zarić SD (2013) σ-Hole interactions of covalently-bonded nitrogen, phosphorus and arsenic: a survey of crystal structures. Crystal 4:12–31
28. Bleiholder C, Werz DB, Köppel H, Gleiter R (2006) Theoretical investigations on chalcogen-chalcogen interactions: what makes these nonbonded interactions bonding? J Am Chem Soc 128:2666–2674
29. Zhang Y, Wang W (2009) The bifurcate chalcogen bond: some theoretical observations. J Mol Struct (THEOCHEM) 916:135–138
30. Esrafili MD, Vakili M, Solimannejad M (2014) Cooperative interaction between π-hole and single-electron σ-hole interactions in $O_2S\cdots NCX\cdots CH_3$ and $O_2Se\cdots NCX\cdots CH_3$ complexes (X=F, Cl, Br and I). Mol Phys 112:2078–2084
31. Brezgunova ME, Lieffrig J, Aubert E, Dahaoui S, Fertey P, Lebègue S, Ángyán JG, Fourmigué M, Espinosa E (2013) Chalcogen bonding: experimental and theoretical determinations from electron density analysis. Geometrical preferences driven by electrophilic–nucleophilic interactions. Cryst Growth Des 13:3283–3289
32. Saczewski J, Frontera A, Gdaniec M, Brzozowski Z, Saczewski F, Tabin P, Quiñonero D, Deyà PM (2006) Synthesis, X-ray structure analysis and computational studies of novel bis(thiocarbamoyl) disulfides with non-covalent S···N and S···S interactions. Chem Phys Lett 422:234–239
33. Bauzá A, Quiñonero D, Deyà PM, Frontera A (2013) Halogen bonding versus chalcogen and pnicogen bonding: a combined Cambridge structural database and theoretical study. Cryst Eng Comm 15:3137–3144
34. Wang W, Ji B, Zhang Y (2009) Chalcogen bond: a sister noncovalent bond to halogen bond. J Phys Chem A 113:8132–8135
35. Iwaoka M, Takemoto S, Tomoda S (2002) Statistical and theoretical investigations on the directionality of nonbonded S···O interactions. Implications for molecular design and protein engineering. J Am Chem Soc 124:10613–10620
36. Dahaoui S, Pichon-Pesme V, Howard JAK, Lecomte C (1999) CCD charge density study on crystals with large unit cell parameters: the case of hexagonal l-cystine. J Phys Chem A 103:6240–6250
37. Lee CR, Tang TH, Chen L, Wang CC, Wang Y (2004) Topological analysis of charge density in heptasulfur imide (S7NH) from isolated molecule to solid. J Phys Chem Solids 65:1957–1966
38. Scheiner S (2013) Detailed comparison of the pnicogen bond with chalcogen, halogen, and hydrogen bonds. Int J Quantum Chem 113: 1609–1620
39. Li QZ, Li R, Guo P, Li H, Li WZ, Cheng JB (2012) Competition of chalcogen bond, halogen bond, and hydrogen bond in SCSAHOX and SeCSe–HOX (X=Cl and Br) complexes. Comput Theor Chem 980:56–61
40. Cozzolino AF, Vargas-Baca I, Mansour S, Mahmoudkhani AH (2005) The nature of the supramolecular association of 1,2,5-chalcogenadiazoles. J Am Chem Soc 127:3184–3190
41. Solimannejad M, Gharabaghi M, Scheiner S (2011) SH···N and SH···P blue-shifting H-bonds and N···P interactions in complexes pairing HSN with amines and phosphines. J Chem Phys 134:024312
42. Scheiner S (2011) A new noncovalent force: comparison of P···N interaction with hydrogen and halogen bonds. J Chem Phys 134: 094315

43. Scheiner S (2011) Effects of substituents upon the P···N noncovalent interaction: the limits of its strength. J Phys Chem A 115:11202–11209
44. Adhikari U, Scheiner S (2012) Sensitivity of pnicogen, chalcogen, halogen and H-bonds to angular distortions. Chem Phys Lett 532:31–35
45. Scheiner S (2011) Can two trivalent N atoms engage in a direct N···N noncovalent interaction? Chem Phys Lett 514:32–35
46. Alkorta I, Elguero J, Del Bene JE (2013) Pnicogen-bonded cyclic trimers $(PH_2X)_3$ with X=F, Cl, OH, NC, CN, CH_3, H, and BH_2. J Phys Chem A 117:4981–4987
47. Zahn S, Frank R, Hey-Hawkins E, Kirchner B (2011) Pnicogen bonds: a new molecular linker? Chem Eur J 17:6034–6038
48. Vickaryous WJ, Healy ER, Berryman OB, Johnson DW (2005) Synthesis and characterization of two isomeric, self-assembled arsenic–thiolate macrocycles. Inorg Chem 44:9247–9252
49. Saparov B, He H, Zhang X, Greene R, Bobev S (2010) Synthesis, crystallographic and theoretical studies of the new Zintl phases $Ba_2Cd_2Pn_3$ (Pn=As, Sb), and the solid solutions $(Ba_{1-x}Sr_x)_2Cd_2Sb_3$ and $Ba_2Cd_2(Sb_{1-x}As_x)_3$. Dalton Trans 39:1063–1070
50. Solimannejad M, Ghafari S, Esrafili MD (2013) Theoretical insight into cooperativity in lithium-bonded complexes: linear clusters of LiCN and LiNC. Chem Phys Lett 577:6–10
51. Esrafili MD, Shahabivand S (2014) A theoretical evidence for cooperativity effects in fluorine-centered halogen bonds: linear $(FCN)_{2-7}$ and $(FNC)_{2-7}$ clusters. Struct Chem 25:403–408
52. Esrafili MD, Mohammdian-Sabet F, Esmailpour P (2013) Theoretical study on cooperative effects between X···N and X···carbene halogen bonds (X=F, Cl, Br and I). J Mol Model 19:4797–4804
53. Esrafili MD, Esmailpour P, Mohammadian F, Solimannejad M (2013) Theoretical study of the interplay between halogen bond and lithium–π interactions: cooperative and diminutive effects. Chem Phys Lett 588:47–50
54. McDowell SAC, Yarde HK (2012) Cooperative effects of hydrogen, lithium and halogen bonding on F–H/Li···OH_2 complexes. Phys Chem Chem Phys 14:6883–6888
55. Liu X, Cheng J, Li Q, Li W (2013) Competition of hydrogen, halogen, and pnicogen bonds in the complexes of HArF with XH_2P (X=F, Cl, and Br). Spectrochim Acta A 101:172–177
56. McDowell SAC, Buckingham AD (2014) Cooperative effects in FH/Li···HCCX···OH_2 complexes (X=F,Cl,Br,H). Spectrochim Acta A 136PA:27–31. doi: 10.1016/j.saa.2013.10.056
57. George J, Deringer VL, Dronskowski R (2014) Cooperativity of halogen, chalcogen, and pnictogen bonds in finite molecular chains by electronic structure theory. J Phys Chem A 118:3193–3200
58. Esrafili MD, Vakili M, Solimannejad M (2014) Cooperative effects in pnicogen bonding: $(PH_2F)_{2-7}$ and $(PH_2Cl)_{2-7}$ clusters. Chem Phys Lett 609:37–41
59. Li QZ, Li R, Liu XF, Li WZ, Cheng JB (2012) Concerted interaction between pnicogen and halogen bonds in XCl–FH_2P–NH_3 (X=F, OH, CN, NC, and FCC). Chem Phys Chem 13:1205–1212
60. Esrafili MD, Vakili M, Solimannejad M (2014) Cooperativity effects between σ-hole interactions: a theoretical evidence for mutual influence between chalcogen bond and halogen bond interactions in F_2S···NCX···NCY complexes (X=F, Cl, Br, I; Y=H, F, OH). Mol Phys 112:2078–2084
61. Schmidt MW, Baldridge KK, Boatz JA, Elbert ST, Gordon MS, Jensen JH, Koseki S, Matsunaga N, Nguyen KA, Su SJ, Windus TL, Dupuis M, Montgomery JA (1993) General atomic and molecular electronic structure system. J Comput Chem 14:1347–1363
62. Boys SF, Bernardi F (1970) The calculation of small molecular interactions by the differences of separate total energies. Some procedures with reduced errors. Mol Phys 19:553–566
63. Su P, Li H (2009) Energy decomposition analysis of covalent bonds and intermolecular interactions. J Chem Phys 131:014102
64. Xantheas SS (2000) Cooperativity and hydrogen bonding network in water clusters. Chem Phys 258:225–231
65. Bulat FA, Toro-Labbe A, Brinck T, Murray JS, Politzer P (2010) Quantitative analysis of molecular surfaces: areas, volumes, electrostatic potentials and average local ionization energies. J Mol Model 16:1679–1691
66. Wolinski K, Hilton JF, Pulay P (1990) Efficient implementation of the gauge-independent atomic orbital method for NMR chemical shift calculations. J Am Chem Soc 112:8251–8260
67. Ho PS (2014) Biomolecular halogen bonds. Top Curr Chem. doi: 10.1007/128_2014_551
68. Li Q, Zhu H, Zhuo H, Yang X, Li W, Cheng J (2014) Complexes between hypohalous acids and phosphine derivatives. Pnicogen bond versus halogen bond versus hydrogen bond. Spectrochim Acta A 132:271–277
69. Kleeberg H, Klein D, Luck WAP (1987) Quantitative infrared-spectroscopic investigations of hydrogen-bond cooperativity. J Phys Chem 91:3200–3203
70. Li Q, Lin Q, Li W, Cheng J, Gong B, Sun J (2008) Cooperativity between the halogen bond and the hydrogen bond in H3N···XY···HF complexes (X, Y=F, Cl, Br). Chem Phys Chem 9:2265–2269